IEEE Access
Multidisciplinary | Rapid Review | Open Access Journal

Received August 31, 2020, accepted September 9, 2020, date of publication September 18, 2020, date of current version October 1, 2020.

Digital Object Identifier 10.1109/ACCESS.2020.3024931

Optimal Dispatching Strategy of an Electric-Thermal-Gas Coupling Microgrid Considering Consumer Satisfaction

HAILIANG XU, (Member, IEEE), ZHIYUAN MENG, RENDE ZHAO, (Member, IEEE), YANSONG WANG, AND QINGZENG YAN

College of New Energy, China University of Petroleum (East China), Qingdao 266580, China

Corresponding author: Hailiang Xu (xuhl@zju.edu.cn)

This work was supported in part by the Fundamental Research Funds for the Central Universities under Grant 19CX02016A, and in part by the Key Research and Development Project of Shandong Province under Grant 2019GGX103045.

ABSTRACT In recent years, with the rapid development of renewable energy, microgrid that behaves as a multi-energy coupling system, has attracted more and more attention. A growing trend needs to be concerned is that the relation among the electric power, thermal and gas in a microgrid system gets closer and closer, which could significantly affect the system dispatching. The existing research on microgrid dispatch mainly focuses on power and load coordination and improving the utilization rate of primary energy. However, there is some limit in the energy form independence and operation mode. Besides, some research had ignored the consumer electricity experience in load optimization. To settle such problem, a dispatching model based on a complicated electric-thermal-gas coupling microgrid is firstly proposed in this paper. Then the mathematical model of the subsystems in the microgrid is established, and the demand side response based on consumer satisfaction is employed to optimize the loads. Finally, the operation cost of the microgrid can be minimized by the proposed economic optimization strategy. Case studies were performed to verify the effectiveness of the proposed scheduling strategy.

INDEX TERMS Microgrid, demand side response, electric-thermal-gas coupling, consumer satisfaction.

I. INTRODUCTION

Nowadays, microgrids which include a large number of distributed energy, energy storage equipment and communication systems have become a very important part of the power system [1]–[3]. However, in the earlier years, the energy form of microgrids is quite simple, i.e., only generated and consumed as electric power. This leads to the low utilization of resources, and also poses new challenge to the dispatch issue [4]–[7]. To settle this problem, in [8] an electric-thermal coupling dispatching model is established which realizes the full utilization of electric energy and thermal energy, and thus reduces the operating cost of the microgrid. In [9], a microgrid system that combined cooling, heating and electric power is presented, based on which a peak-adjusting strategy is proposed by considering the prediction errors of load and photovoltaic (PV). However, the method in [8] only takes the combination of electricity and heat into account, but does not consider the cooling load. In [9], though the cooling, heating and power are combined, its optimization objective only focus on the fuel cost and electricity price, leaving the load-side behavior irrespective.

In fact, the demand side response has been recognized as an important factor in the microgrid dispatching process. Through reasonable classification and guidance of the loads, their reduction or transfer can be realized to reduce the load fluctuation. Besides, when the load transfer is combined with time of use (TOU) price and consumer satisfaction, it is really beneficial to the economy and power users [10]–[12]. In [13], the electrical loads are divided into two categories, i.e., the interruptible loads and the transferrable ones, where a demand side response model is presented. Computer simulations verified that it can reduce the operating cost of the microgrid. In [14], taking the electric-thermal coupling system as the background, an elastic demand side response model is established to optimize the load scheduling, proving that the it can cut down the system operating cost and improve the absorption capacity of PVs as well. However,

The associate editor coordinating the review of this manuscript and approving it for publication was Bin Zhou.

it needs to point out that when scheduling the loads, not only the economic factors should be considered, but also the satisfaction of the consumers ought to be thought over. Note that in [13] and [14], the consumer satisfaction affected by the demand side response had not been considered, which in fact, plays an important role in the dispatching design of a microgrid.

As a specific contribution, this paper proposes an optimal dispatching strategy for the complicated electric-thermal-gas coupling microgrid, taking the consumer satisfaction into consideration. To do so, the optimizing scheduling model of the microgrid has been established in detail, and solved by the particle swarm optimization algorithm (PSO). The following part of this paper is organized as follows. Section II presents the modeling of the electric-thermal-gas coupling microgrid. Then the demand side response model that considers consumer satisfaction is established in Section III. In Section IV, an economic dispatching strategy is put forward, and its effectiveness is thus verified by case studies in Section V. Finally, Section VI concludes the findings.

II. MODELING OF THE ELECTRIC-THERMAL-GAS COUPLING MICROGRID

A. MICROGRID CONFIGURATION

The basic configuration of the electricity-thermal-gas coupling microgrid is shown in Fig. 1. The grid-connected distributed power supplies are composed of the gas turbine, internal combustion engine, gas boiler, heat recovery system, hot cooler, electric cooler, wind power generation, photovoltaic and battery. As shown, the loads includes the electric load, cooling load, heat load and gas load.

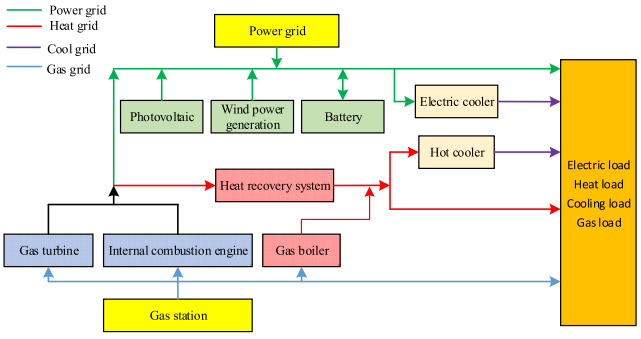

FIGURE 1. Configuration of the electric-thermal-gas coupling microgrid.

B. MATHEMATICAL MODEL OF GAS TURBINE AND INTERNAL COMBUSTION ENGINE

The mathematical model of gas turbine, internal combustion engine are given in [15, 16]. Their mathematical model can be represented as

$$\eta_{GT}(t) = A_{GT} + B_{GT} * \frac{P_{GT,e}(t)}{P_{GTN}} + C_{GM} * \left(\frac{P_{GT,e}(t)}{P_{GTN}}\right)^2 + D_{GT} * \left(\frac{P_{GT,e}(t)}{P_{GTN}}\right)^3 \quad (1)$$

$$\eta_{CE}(t) = A_{CE} + B_{CE} * \frac{P_{CE,e}(t)}{P_{CEN}} + C_{CE} * \left(\frac{P_{CE,e}(t)}{P_{CEN}}\right)^2 + D_{CE} * \left(\frac{P_{CE,e}(t)}{P_{CEN}}\right)^3 \quad (2)$$

where $\eta_{GT}(t)$ and $\eta_{CE}(t)$ are the efficiency of the gas turbine and internal combustion engine at time t; $P_{GT}(t)$ and $P_{CE,e}(t)$ are their output electric power at time t; P_{GTN} and P_{CEN} represent their rated power; A_{GT}-D_{GT} and A_{CE}-D_{CE} stand for the efficiency parameters.

The operation cost model can then be expressed as

$$\begin{aligned} C_{GT}(t) &= CF_{GT}(t) + CO_{GT}(t) + CM_{GT}(t) \\ &= C_{ng} \times \frac{P_{GT}(t)}{\eta_{GT}(t)} + K_{COGT} \times P_{GT}(t) \\ &\quad + \sum_{k=1}^{M} \alpha k \times \lambda k_{GT} \times P_{GT}(t) \end{aligned} \quad (3)$$

$$\begin{aligned} C_{CE}(t) &= CF_{CE}(t) + CO_{CE}(t) + CM_{CE}(t) \\ &= C_{ng} \times \frac{P_{CE}(t)}{\eta_{CE}(t)} + K_{COCE} \times P_{CE}(t) \\ &\quad + \sum_{k=1}^{M} \alpha k \times \lambda k_{CE} \times P_{CE}(t) \end{aligned} \quad (4)$$

where $C_{GT}(t)$ and $C_{CE}(t)$ stand for the operation cost of the gas turbine and internal combustion engine at time t; $CF_{GT}(t)$ and $CF_{CE}(t)$ are gas cost; $CO_{GT}(t)$ and $CO_{CE}(t)$ are maintenance cost; $CM_{GT}(t)$ and $CM_{CE}(t)$ are environmental cost; C_{ng} denotes the price of the gas; K_{COGT} and K_{COCE} are the proportionality constant of maintenance cost; αk is the discounted cost; λk_{GT} and λk_{CE} are the emission coefficient; M stands for the pollution type. Here, the pollution types of the NO_x, SO_2 and CO_2 are considered.

Fig. 1 shows that gas turbine and internal combustion engine generate heat while generating electricity, their heating model can then be given as

$$P_{GT,h}(t) = \frac{P_{GT}(t)}{\eta_{GT}(t)} \times (1 - \eta_{GT}(t) - \eta_{l,GT}) \quad (5)$$

$$P_{CE,h}(t) = \frac{P_{CE}(t)}{\eta_{CE}(t)} \times (1 - \eta_{CE}(t) - \eta_{l,CE}) \quad (6)$$

where $P_{GT,h}(t)$ and $P_{CE,h}(t)$ are heat production of gas turbine and internal combustion engine at time t; $\eta_{l,GT}$ and $\eta_{l,CE}$ are the heat loss coefficient.

C. MATHEMATICAL MODEL OF BATTERY

The charging and discharging model of the battery can be expressed as [17]

$$C(t+1) = (1 - \eta_{ST,s})C(t) + d_d \frac{P_t^{ST,d}}{\eta_{ST,d}} + d_c \frac{P_t^{ST,c}}{\eta_{ST,c}} \quad (7)$$

where $C(t)$ is the energy stored in the battery at time t; d_d and d_c indicate the discharge and charge respectively, i.e., when the battery is charged, $d_d = 0$, $d_c = 1$, and when the battery is discharged, $d_d = 1$, $d_c = 0$; $P_t^{ST,d}$ and $P_t^{ST,c}$ are respectively the discharge and charging power of the battery at time t, and the charging power is negative, while the discharging power

is positive; $\eta_{ST,s}$ is the self discharge rate of the battery; $\eta_{ST,d}$ and $\eta_{ST,c}$ are the discharge and charging efficiency of the battery, respectively.

The battery maintenance cost model can then be expressed by

$$CO_{ST}(t) = K_{COST} \times |P_{ST}(t)| + (C_M C_i + P_{STM} C_P) H_{ST}(t) \tag{8}$$

where $CO_{ST}(t)$ is the maintenance cost of battery; K_{COST} is the proportionality constant of maintenance cost; $P_{ST}(t)$ is charging or discharging power of the battery; C_M denotes the nominal capacity of the battery; C_i is the installation cost per unit capacity of the battery; P_{STM} is the rated power of the battery; C_P is the unit power installation cost of the battery; $H_{ST}(t)$ stands for battery life loss function, which can be expressed as follows:

$$H_{ST}(t) = \frac{C_{loss}(t)}{C_{MOUT}} \tag{9}$$

$$C_{loss}(t) = |P_{ST}(t)| \times f(SOC) \tag{10}$$

where C_{MOUT} is the total energy throughput of the battery in its service life, which can be given by the manufacturer; $C_{loss}(t)$ is the energy of the battery in a certain dispatching period; SOC is the charged state of the battery; $f(SOC)$ is the weight coefficient of battery life loss, as depicted in Fig. 2.

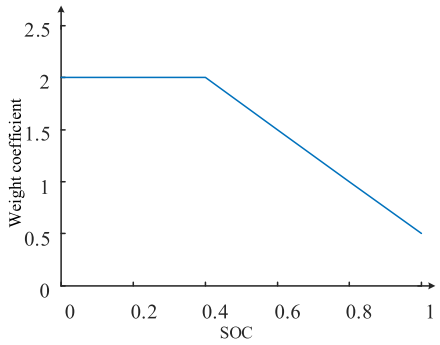

FIGURE 2. Battery life loss weight coefficient curve.

D. MATHEMATICAL MODEL OF POWER PURCHASE

The mathematical model of power purchase can be represented as

$$C_p(t) = \rho_p(t) \times P_p(t) \tag{11}$$

where $\rho_p(t)$ is the electricity price at time t; $P_p(t)$ is the power purchase at time t; when the microgrid purchases electricity from the grid, $P_p(t)$ represents a positive number, while microgrid sells electricity to the grid, it represents as a negative number.

E. MATHEMATICAL MODEL OF THE REST OF THE EQUIPMENT

The mathematical model of the gas boiler can be represented as

$$P_{GB,h}(t) = \eta_{GB} P_{GB,g}(t) \tag{12}$$

where $P_{GB,h}(t)$ represents the heat power output by the gas boiler at time t; η_{GB} indicates the efficiency of the heat generation; $P_{GB,g}(t)$ is the gas input to the gas boiler.

The operation cost model can then be expressed as

$$\begin{aligned} C_{GB}(t) &= CF_{GB}(t) + CO_{GB}(t) \\ &= C_{ng} \times P_{GB,g}(t) + K_{COGB} \times P_{GB,h}(t) \end{aligned} \tag{13}$$

where $C_{GB}(t)$ stands for the operation cost of the gas boiler at time t; $CF_{GB}(t)$ is gas cost; $CO_{GB}(t)$ is maintenance cost; K_{COGB} is the proportionality constant of maintenance cost.

The mathematical model of the heat recovery system, electric cooler and hot cooler can be referred to (12), which are given as below

$$P_{HR,h}(t) = \eta_{HR,h} P_{HR,ih}(t) \tag{14}$$

$$P_{EC,c}(t) = CR_{EC} P_{EC,ie}(t) \tag{15}$$

$$P_{HC,c}(t) = CR_{HC} P_{HC,ih}(t) \tag{16}$$

In (14)-(16), $P_{HR,h}(t)$, $P_{EC,c}(t)$ and $P_{HC,c}(t)$ respectively stand for heat power output by heat recovery system, and cool power output by electric cooler and hot cooler; $P_{HR,ih}(t)$ is heat power input to the heat recovery system; $P_{EC,ie}(t)$ is electric power input to the electric cooler; $P_{HC,ih}(t)$ is heat power input to the hot cooler; $\eta_{HR,h}$ represents the efficiency of the heat recovery system; CR_{EC} and CR_{HC} represent the refrigeration coefficient of electric cooler and hot cooler respectively.

The operating cost of the heat recovery system, electric cooler and hot cooler are mainly the maintenance cost, which can be expressed as

$$CO_{HR}(t) = K_{COHR} \times P_{HR,h}(t) \tag{17}$$

$$CO_{EC}(t) = K_{COEC} \times P_{EC,c}(t) \tag{18}$$

$$CO_{HC}(t) = K_{COHC} \times P_{HC,c}(t) \tag{19}$$

where $CO_{HR}(t)$, $CO_{EC}(t)$ and $CO_{HC}(t)$ represent the maintenance cost of the heat recovery system, electric cooler and hot cooler respectively; K_{COHR}, K_{COEC} and K_{COHC} are the proportionality constant of maintenance cost.

F. MODEL CONSTRAINTS

The constraints of the microgrid can be given as below:

$$\begin{aligned} E_L(t) &= P_{GT,e}(t) + P_{CE,e}(t) + P_{ST}(t) \\ &\quad + P_{WT}(t) + P_{PV}(t) + P_p(t) - P_{EC,ie}(t) \end{aligned} \tag{20}$$

$$H_L(t) = P_{HR,h}(t) + P_{GB,h}(t) - P_{HC,ih}(t) \tag{21}$$

$$C_L(t) = P_{EC,c}(t) + P_{HC,c}(t) \tag{22}$$

$$P_i^{\min} \le Pi(t) \le P_i^{\max} \tag{23}$$

$$\left|P_{grid}(t)\right| \le P_{grid}^{\max} \tag{24}$$

$$SOC\ \min \le SOC(t) \le SOC\ \max \tag{25}$$

$$SOC(t) = \frac{C(t)}{C_M} \times 100\% \tag{26}$$

In (20)-(26), (20) represents the electrical power balance of the microgrid, (21) represents the heat power balance and (22) is the cool power balance, $E_L(t)$, $H_L(t)$ and $C_L(t)$ are

electrical load, heat load and cooling load; (23) represents the output constraint of the equipment in microgrid; (24) represents the capacity constraint of the tie line with the power grid; (25) and (26) stand for the SOC constraints of the battery; $C(t)$ denotes the capacity of the battery at time t.

III. DEMAND SIDE RESPONSE MODEL THAT CONSIDERS CONSUMER SATISFACTION

In the demand side model, the electrical loads can be divided into the schedulable and the non-schedulable ones [18]. And the non-schedulable part can be regarded as the basic load of the microgrid. As for the schedulable ones, it can further be classified into the transferrable load and interruptible loads.

The mathematical models of transferrable and interruptible loads can be respectively expressed as [19]

$$\sum_{t=1}^{T} P_{\text{tran,k}} = P_{T,\text{k}} \tag{27}$$

$$P_{\text{int,t}} = \sum_{\text{k}=1}^{N_{\text{cut}}} \text{S}_{\text{k,t}} P_{\text{int,k,t}} \tag{28}$$

In (27) and (28), $P_{\text{tran,k}}$ represents the value of class k transferable load at time t; $PT_{,\text{k}}$ represents the total amount of class k transferable load.; $P_{\text{int,t}}$ is the reduction of interruptible load at time t; $P_{\text{int,k,t}}$ is the load of class interruptible load at time t; N_{cut} is the number of types of interruptible loads; $\text{S}_{\text{k,t}}$ is the reduction of class k interruptible load at time t, where 1 means reduced, 0 means un-reduced.

As for the load optimization, the consumer satisfaction can be expressed by electricity price, electricity consumption and load reduction before and after demand side response [20]. Thus, the consumer satisfaction can be given as below

$$\begin{aligned} S_{\text{L}} &= S_{\text{es}} + S_{\text{eL}} + S_{\text{int}} \\ &= \left(1 - \frac{\sum_{t=1}^{T} \Delta C_{\text{pl}}(t)}{\sum_{t=1}^{T} C_{\text{pl}}(t)}\right) + \left(1 - \frac{\sum_{t=1}^{T} |\Delta d_{\text{p}}(t)|}{\sum_{t=1}^{T} d_{\text{p}}(t)}\right) \\ &\quad + \left(1 - \frac{\sum_{t=1}^{T} |\Delta P_{\text{int,t}}|}{\sum_{t=1}^{T} P_{\text{INT,t}}}\right) \end{aligned} \tag{29}$$

$$C_{\text{pl}}(t) = d_{\text{p}}(t) \cdot \rho_{\text{p}}(t) \tag{30}$$

$$\Delta C_{\text{pl}}(t) = \Delta d_{\text{p}}(t) \cdot \rho_{\text{p}}(t) \tag{31}$$

In (29)-(31), S_{L} stands for the satisfaction of the consumer; S_{es} represents the satisfaction degree of electricity purchase; $C_{\text{pl}}(t)$ represents the electricity purchase price before demand side response and $\Delta C_{\text{pl}}(t)$ is the change of electricity purchase price before and after the demand side response at time t; $\rho_{\text{p}}(t)$ is the electricity price; S_{eL} is the satisfaction degree of load transfer; $d_{\text{p}}(t)$ is the electricity consumption before the demand side response; $\Delta d_{\text{p}}(t)$ is the change of electricity consumption before and after the demand side response; S_{int} is the consumer satisfaction with load reduction; $\Delta P_{\text{int,t}}$ is the change of interruptible load; $P_{\text{INT,t}}$ is the load of interruptible load before demand side response.

IV. ECONOMIC DISPATCHING APPROACH

Based on the presented models of the microgrid and the demand side, the optimal dispatching process can be developed according to the objective function.

Considering the customer satisfaction, the objective function in the load side can be established by

$$f(P_{\text{L}}) = \max S_{\text{L}} \tag{32}$$

Meanwhile, on the power side, the optimization goal is to lowest the operating cost of the microgrid, and the objective function can be built up as

$$\begin{aligned} F(P) = \sum_{t=1}^{T} \Bigg[&\sum_{\text{i=1}} CF_{\text{i}}(t) + \sum_{\text{i=1}} CO_{\text{i}}(t) \\ &+ \sum_{\text{i=1}} CM_{\text{i}}(t) + \sum_{\text{i=1}} CG_{\text{i}}(t) \Bigg] \end{aligned} \tag{33}$$

where $CF_{\text{i}}(t)$ is the gas cost; $CO_{\text{i}}(t)$ is the maintenance cost; $CM_{\text{i}}(t)$ is the environmental cost; $CG_{\text{i}}(t)$ is the power purchase cost; i represents the type of equipment.

The proposed economic dispatching flow chart of the microgrid is shown detailedly in Fig. 3, which can be summarized as follows:

Step 1: According to the load data of microgrid system, the output limitation and algorithm parameters of each equipment are firstly determined.

Step 2: The electrical load is then divided into three parts: the important load, transferable load and interruptible load.

Step 3: Based on the load prediction results and (32), optimize the electric load with the highest consumer satisfaction.

TABLE 1. Time of use of the electricity price.

	Peak period (9h-12h, 15h-19h)	Flat period (7h-8h, 13h-14h, 20h-22h)	Valley period (1h-6h, 23h-24h)
Power purchase (cents/kWh)	12.21	8.42	4.87
Sell electricity (cents/kWh)	10.55	6.39	2.53

Step 4: Before carrying out the economic optimization, it is necessary to arrange the battery dispatching strategy combining the TOU electricity price and load optimization results. Tab. 1 shows the TOU electricity price under these periods. As can be seen from Tab. 1, when the microgrid is in the peak period, the power purchase price is high, so the battery should discharge to reduce the power purchase. When the microgrid enters the flat period and valley period with low electricity price, the battery can decide whether to charge according to its own SOC.

Step 5: According to the load curve obtained in Step 3 and the working state of battery in Step 4, the economic dispatching of microgrid can be carried out. In the dispatch process, priority is given to the consumption of wind power and PVs, and the purchase of electricity is reasonably arranged according to the electricity price.

V. CASE STUDIES

To verify the effectiveness of the proposed dispatch strategy, case studies are performed with its configuration shown in Fig. 1. The grid-connected microgrid coupling electric-thermal-gas consists of wind power, PVs, battery, electric-thermal systems and other equipment. The scheduling cycle is 24h, and the unit scheduling time is 1h. The parameters of some equipment are shown in Tab. 2, where P_M is the rated power; P_{max} means maximum power and P_{min} is minimum power. Among these power parameters, the electrical power features for the gas turbine, internal combustion engine, power grid and battery, while the heat power characterizes the gas boiler and heat recovery system.

TABLE 2. Relevant parameters of microgrid equipment.

The equipment parameters	P_M/kW	P_{max}/kW	P_{min}/kW
Gas turbine	4500	4600	500
Internal combustion engine	3500	3550	300
Power grid	—	2000	-2000
Battery	1500	1500	-1500
Gas boiler	4000	4000	500
Heat recovery system	4000	4100	—

A. DISPATCH RESULT ANALYSIS

According to the flow chart in Fig. 3, the scheduling of the microgrid can be optimized under the grid-connected

operation mode. The curves of the initial daily load and renewable energy are shown in Fig. 4, while the dispatching results are presented in Fig. 5.

Comparing Figs. 4 and 5, it can be concluded that the electrical load is significantly reduced in the peak period when the proposed strategy is adopted, i.e., part of the transferrable load is shifted to the flat and valley period which time the electricity price is much lower. Affected by consumer satisfaction, the transferrable load cannot be transferred out of peak period completely, and the reduction amount of interruptible load in peak period is lower than that in other periods.

Besides, based on the load optimization curve obtained in Fig. 5, the economic dispatching of the microgrid can be explored. The economic scheduling results are displayed in Fig. 7 and the results before the demand side response are presented in Fig. 6.

By comparing Figs. 6 and 7, it can also be seen that the electric load during 9h-12h is reduced when the demand side

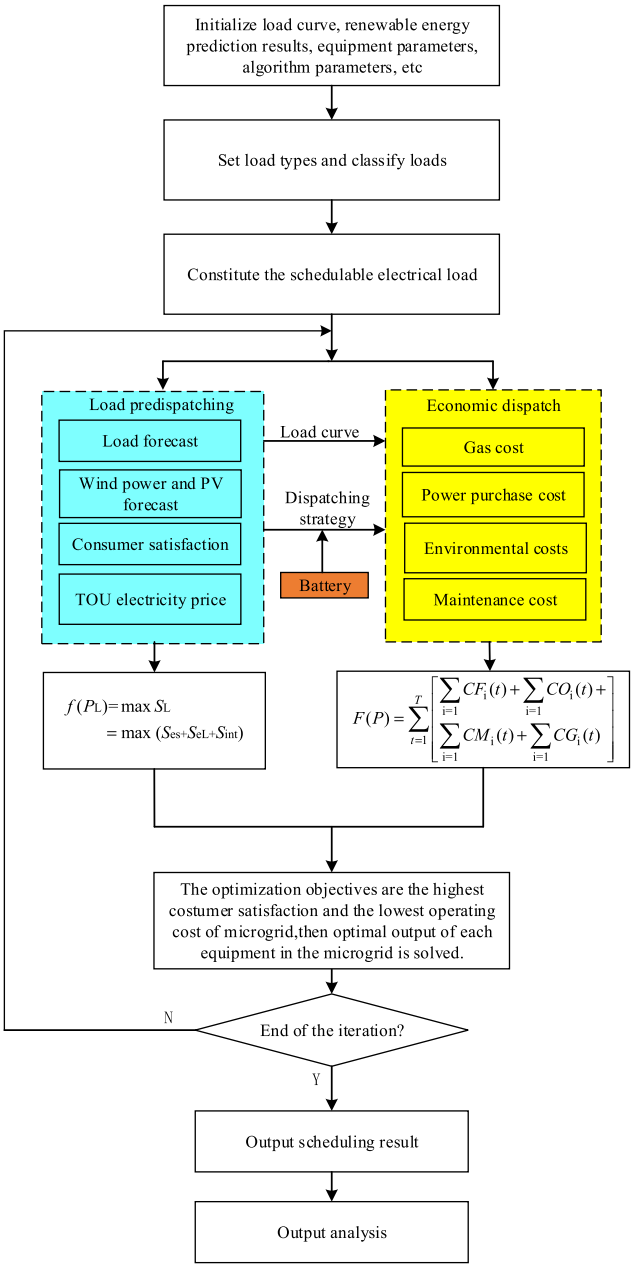

FIGURE 3. Dispatch process of the microgrid.

response is adopted, which reduces the generation capacity of gas turbine and internal combustion engine and is conducive to the reduction of operating cost. During 1h-6h, the microgrid is in the valley period, under the influence of the demand side, the electrical load at this stage increases slightly, resulting in the increase the output of the internal combustion engine. However, the electricity price and gas price are lower in the valley period and flat period, so it has little increase in the operation cost.

The variation of power generation capacity of each generation equipment in the microgrid before and after the demand side response is exhibited in Fig. 8. As can be seen from Fig. 8, as the main power generation equipment,

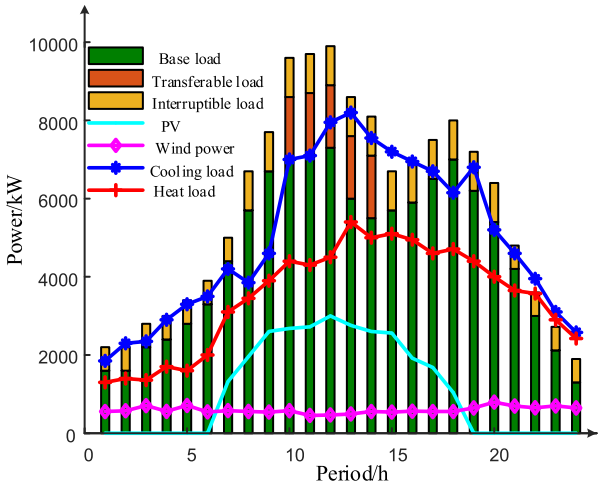

FIGURE 4. Daily load forecasting curve.

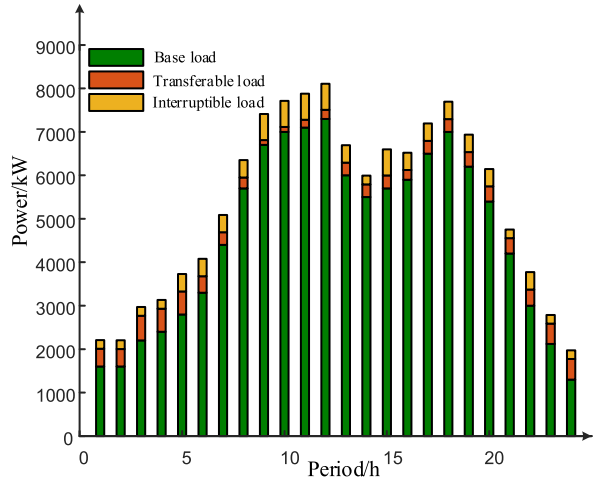

FIGURE 5. Load optimization curve.

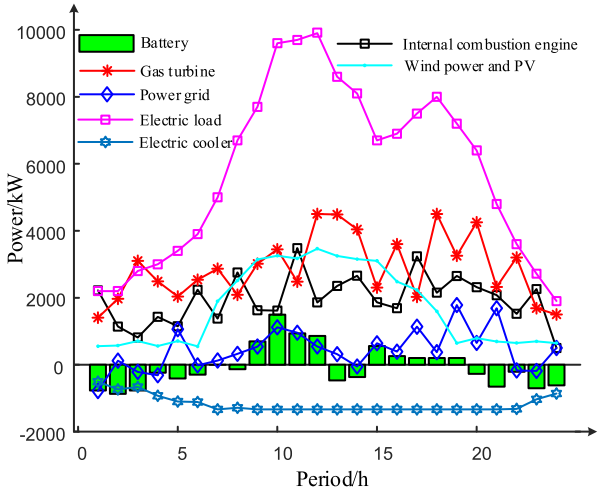

FIGURE 6. Economic dispatch result before the demand side response.

the generation capacity of internal combustion engine and gas turbine decreases to a large extent after the adoption of demand side response. Since the capacity and cost of tie lines and batteries are low, their variation is not so significant.

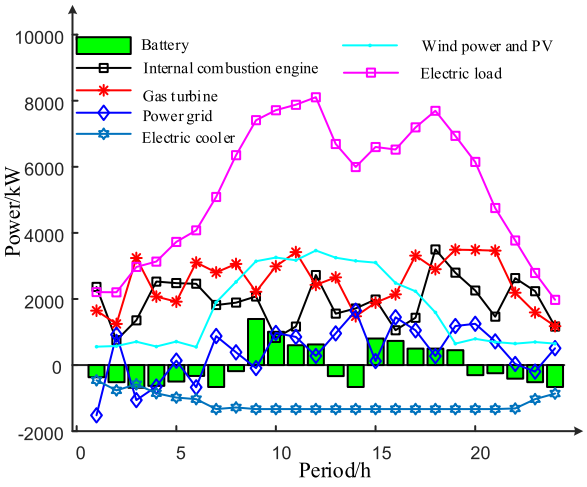

FIGURE 7. Economic dispatch result after the demand side response.

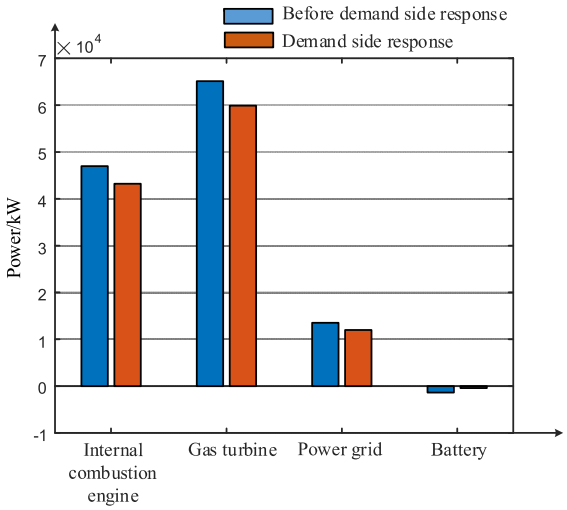

FIGURE 8. Changes in the power generation of equipment.

As for the working state of the battery, Fig. 9 shows the changes of the SOC in a day after using the demand side response. According to Fig. 3 and (25), it can be seen that its output is related to the electricity price and SOC. Therefore, in Figs. 7 and 9, due to the low initial capacity of the battery, the battery is charged during the valley period and the flat period when the electricity price is low; at the time interval of 9h-12h, the microgrid is in peak period, and the electricity price is the highest. Therefore, according to the scheduling strategy, the battery needs to be discharged to reduce the amount of electricity purchased; during 13h-14h, the micogrid gets into the flat period again. Since in the peak period the battery has released more electric quantity, and its SOC has reached the limit value, it turns into the charging mode. The working state of the battery in the later period of time is similar to before, but the output power is reduced. It can be seen from Fig. 9 that after the end of the first peak period, the SOC of the battery significantly decreases. And as can be seen from Fig. 2, when the SOC of the battery is low, its weight coefficient is higher, so the cost gets high. Therefore,

the battery in the later period of time reduces its output power to decline the operating cost.

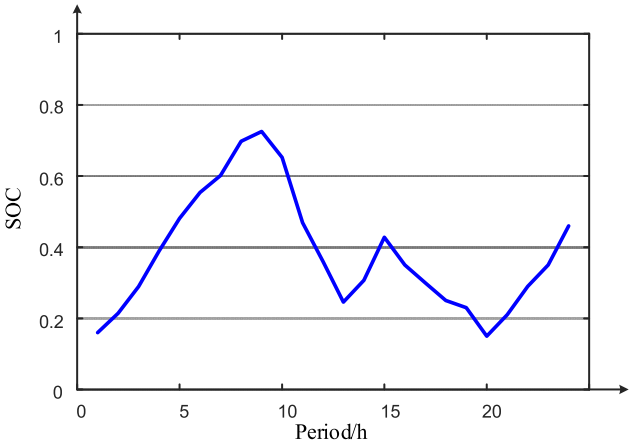

FIGURE 9. SOC of battery after demand side response.

B. MICROGRID OPERATION COST ANALYSIS

The demand side response can not only reduce electricity consumption, but also has a great impact on the reduction of operating cost of the microgrid. Tab. 3 shows the economic costs of electricity-thermal-gas coupling microgrid with and without the proposed dispatch strategy.

TABLE 3. Economic cost of the microgrid.

Dispatch strategy	Gas cost /dollars	Power purchase cost /dollars	Environ-mental cost /dollars	Main-tenance cost /dollars	Total /dollars
Before demand side response	8933.08	1342.71	68.51	70.36	10414.66
Demand side response	8620.29	1258.46	62.38	60.19	10001.32

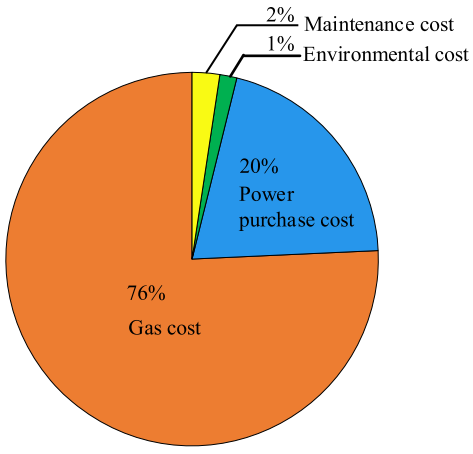

FIGURE 10. Contribution of each part to the cost reduction.

As can be seen in Tab. 3, all costs of the system have been reduced after the adoption of demand side response. To give a clear illustration, the contribution of each part to the cost reduction is shown in Fig. 10. Combined with Figs. 8 and 10, it can be concluded that the main reduction of operation cost comes from the gas cost, since the gas turbines and internal combustion are the main generators of electricity in the microgrid. For the power purchase cost, the adjustment of battery output and the reduction of peak load are the main reasons for its decline.

VI. CONCLUSION

A dispatch strategy considering consumer satisfaction is put forward for the electricity-thermal-gas coupling microgrid in this paper. Simulation results are carried out to verify the effectiveness of the proposed strategy. Some useful conclusions can be summarized as follows.

(1) After the adoption of demand side response, part of the load in the peak period is reduced or transferred to the flat period and valley period with low electricity price, so the peak-valley difference and the overall load of the system are reduced.

(2) Under the corresponding influence of the demand side, the output of power generation equipment in the microgrid decreases, and the total power consumption of the battery also decreases slightly, which has a positive effect on reducing the energy consumption.

(3) The economy impact of demand side response is mainly reflected in the gas cost, since decrease in power generation of major equipment.

However, in this paper, the demand side response is only adopted to the dispatch of electrical load. The cooling load and heat load in the microgrid had not been optimized, resulting in certain limitation in the application of the proposed method. In the near future, we will try to address this deficiency.

REFERENCES

[1] S. Mirsaeidi, X. Dong, S. Shi, and D. Tzelepis, "Challenges, advances and future directions in protection of hybrid AC/DC microgrids," *IET Renew. Power Gener.*, vol. 11, no. 12, pp. 1495–1502, Oct. 2017.

[2] A. H. Hajimiragha, M. R. D. Zadeh, and S. Moazeni, "Microgrids frequency control considerations within the framework of the optimal generation scheduling problem," *IEEE Trans. Smart Grid*, vol. 6, no. 2, pp. 534–547, Mar. 2015.

[3] S. Bahramirad, A. Khodaei, J. Matevson, Z. Li, L. Bertling, E. A. Passo, M. Fotuhi-Firuzabad, "Guest editorial: Special section on asset management in smart grid," *IEEE Trans. Smart Grid*, vol. 6, no. 2, pp. 953–954, Mar. 2015.

[4] G. Mu, M. Yang, D. Wang, G. Yan, and Y. Qi, "Spatial dispersion of wind speeds and its influence on the forecasting error of wind power in a wind farm," *Mod. Power Syst. Clean Energy*, vol. 4, no. 2, pp. 265–274, Apr. 2016.

[5] S. Monesha, S. G. Kumar, and M. Rivera, "Methodologies of energy management and control in microgrid," *IEEE Latin Amer. Trans.*, vol. 16, no. 9, pp. 2345–2353, Sep. 2018.

[6] L. Hernandez, C. Baladron, J. M. Aguiar, B. Carro, A. J. Sanchez-Esguevillas, J. Lloret, and J. Massana, "A survey on electric power demand forecasting: Future trends in smart grids, microgrids and smart buildings," *IEEE Commun. Surveys Tuts.*, vol. 16, no. 3, pp. 1460–1495, Sep. 2014.

[7] H. Han, X. Hou, J. Yang, J. Wu, M. Su, and J. M. Guerrero, "Review of power sharing control strategies for islanding operation of AC microgrids," *IEEE Trans. Smart Grid*, vol. 7, no. 1, pp. 200–215, Jan. 2016.

[8] Z. Li, F. Zhang, J. Liang, Z. Yun, and J. Zhang, "Optimization on microgrid with combined heat and power system," *Proc. CSEE*, vol. 35, no. 14, pp. 3569–3576, Jul. 2015.
[9] Y. Yang, J. Yu, Y, Li, "Optimal load leveling dispatch of CCHP incorporating photovoltaic and storage," *Auto. Electr. Power Sys.*, vol. 41, no. 6, pp. 6–12+29, Mar. 2017.
[10] J. Li, Y. Liu, and L. Wu, "Optimal operation for community-based multi-party microgrid in grid-connected and islanded modes," *IEEE Trans. Smart Grid*, vol. 9, no. 2, pp. 756–765, Mar. 2018.
[11] E. S. Parizy, H. R. Bahrami, and S. Choi, "A low complexity and secure demand response technique for peak load reduction," *IEEE Trans. Smart Grid*, vol. 10, no. 3, pp. 3259–3268, May 2019.
[12] B. Zhang and J. Baillieul, "Control and communication protocols based on packetized direct load control in smart building microgrids," *Proc. IEEE*, vol. 104, no. 4, pp. 837–857, Apr. 2016.
[13] L. Zhu, X. Zhou, X.-P. Zhang, Z. Yan, S. Guo, and L. Tang, "Integrated resources planning in microgrids considering interruptible loads and shiftable loads," *J. Modern Power Syst. Clean Energy*, vol. 6, no. 4, pp. 802–815, Jul. 2018.
[14] C. Dou, X. Zhou, T. Zhang, and S. Xu, "Economic optimization dispatching strategy of microgrid for promoting photoelectric consumption considering cogeneration and demand response," *J. Modern Power Syst. Clean Energy*, vol. 8, no. 3, pp. 557–563, 2020.
[15] J. Liu and J. Li, "A bi-level energy-saving dispatch in smart grid considering interaction between generation and load," *IEEE Trans. Smart Grid*, vol. 6, no. 3, pp. 1443–1452, May 2015.
[16] N. Liu, J. Wang, and L. Wang, "Hybrid energy sharing for multiple microgrids in an integrated Heat–Electricity energy system," *IEEE Trans. Sustain. Energy*, vol. 10, no. 3, pp. 1139–1151, Jul. 2019.
[17] H. Khani and M. R. D. Zadeh, "Real-time optimal dispatch and economic viability of cryogenic energy storage exploiting arbitrage opportunities in an electricity market," *IEEE Trans. Smart Grid*, vol. 6, no. 1, pp. 391–401, Jan. 2015.
[18] T. Logenthiran, D. Srinivasan, and T. Z. Shun, "Demand side management in smart grid using heuristic optimization," *IEEE Trans. Smart Grid*, vol. 3, no. 3, pp. 1244–1252, Sep. 2012.
[19] C. Shao, Y. Ding, J. Wang, and Y. Song, "Modeling and integration of flexible demand in heat and electricity integrated energy system," *IEEE Trans. Sustain. Energy*, vol. 9, no. 1, pp. 361–370, Jan. 2018.
[20] B. Zhao, X. J. Wang, X. S. Zhang, and J. H. Zhou, "Two-layer method of microgrid optimal sizing considering demand-side response and uncertainties," *Trans. China Electrotech. Soci.*, vol. 33, no. 14, pp. 3284–3295, Jul. 2018.

HAILIANG XU (Member, IEEE) received the B.S. degree in electrical engineering from the China University of Petroleum (East China), Qingdao, China, in 2008, and the Ph.D. degree in electrical engineering from Zhejiang University, Hangzhou, China, in 2014.

Since 2018, he has been an Associate Professor with the China University of Petroleum (East China). His current research interests include wind power generation, microgrid, and power quality.

ZHIYUAN MENG received the B.S. degree in electrical engineering from the China University of Petroleum (East China), Qingdao, China, where he is currently pursuing the master's degree. His research interests include power markets and power system optimization, and microgrids.

RENDE ZHAO (Member, IEEE) received the B.S. and M.S. degrees in electrical engineering from Shandong University, Jinan, China, in 1999 and 2002, respectively, and the Ph.D. degree from the College of Electrical Engineering, Hangzhou, China, in 2005.

He was a Visiting Scholar with Aalborg University, Denmark, from 2015 to 2016. Since 2006, he has been with the China University of Petroleum (East China), Qingdao, China. His research interests include renewable energy generation and motor control.

YANSONG WANG received the B.S. degree in electrical engineering from Shandong University, Jinan, China, in 1988, and the M.S. and Ph.D. degrees in electrical engineering from the China University of Petroleum (East China), Qingdao, China, in 1998 and 2005, respectively.

She is currently a Professor with the China University of Petroleum (East China). Her current research interests include power quality analysis, harmonic suppression, power grid optimization planning, power network fault diagnosis, and power load forecasting.

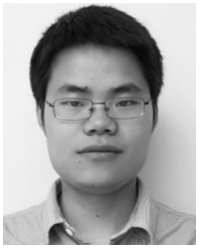

QINGZENG YAN received the B.S. degree in electrical engineering and its automation from the China University of Petroleum (East China), Dongying, China, in 2011, and the Ph.D. degree in electrical engineering from the China University of Mining and Technology, Xuzhou, China, in 2016.

He has been a Lecturer with the College of Information and Control Engineering, China University of Petroleum (East China), Qingdao, China, since 2017. From 2014 and 2016, he was a Visiting Ph.D. Student with the Electrical Energy Management Group (EEMG), University of Bristol, Bristol, U.K., where he was also a Visiting Scholar in 2018. His research interests include power electronics, photovoltaic generation systems, advanced topology and control of multilevel converters, and the applications of wide-bandgap devices.